Colloids and Surfaces B: Biointerfaces 219 (2022) 112813

Contents lists available at ScienceDirect

Colloids and Surfaces B: Biointerfaces

journal homepage: www.elsevier.com/locate/colsurfb

Can polyphenolic surface modifications prevent fungal colonization of titanium dental implants?

Florian Weber [a], Louise Morais Dornelas-Figueira [b], Nora Hafiane [a,c], Daria Zaytseva-Zotova [a], Alejandro Barrantes [d], Fernanda Cristina Petersen [e], Hanna Tiainen [a,*]

[a] Department of Biomaterials, Institute of Clinical Dentistry, University of Oslo, Norway
[b] Universidade Estadual de Campinas Faculdade de Odontologia de Piracicaba, Piracicaba, Brazil
[c] Department of Materials Science, ENSIL-ENSCI, Université de Limoges, France
[d] Oral Research Laboratory, Institute of Clinical Dentistry, University of Oslo, Norway
[e] Institute of Oral Biology, University of Oslo, Norway

ARTICLE INFO

Keywords:
Tannic acid
Pyrogallol
Candida albicans
Saliva
Biofilm

ABSTRACT

Oral biofilms can be a major health problem causing infections and chronic inflammation of mucosal tissue. While much effort is put in the investigation of bacteria in biofilms, the role of fungi is often neglected, despite *Candida albicans* playing a key role in the formation of multispecies oral biofilms. With the rise of antibiotic resistance, new strategies to reduce microbial growth need to be found. Therefore, plant derived polyphenolic molecules have been suggested to reduce both adhesion and growth of pathogenic bacteria and fungi. In this study, we investigated the use of polyphenolic coatings to reduce adhesion and biofilm formation of *C. albicans* BWP17 on titanium implants. Tannic acid and pyrogallol coatings altered the hydrophobic and charge properties of titanium surfaces, and both compounds were gradually released as active molecules over time. Despite such effects, we found no significant inhibition on growth and biofilm formation of *C. Albicans*, indicating that the release of active molecules from the coatings did not reach relevant inhibitory concentrations. However, a potential antibiofilm effect was observed by the pH-dependent disassembly of the polyphenolic layer, which caused the biofilm to detach. Hence, further efforts are required to create tailored implant surfaces, which sustainably reduce microbial growth and adhesion.

1. Introduction

The oral microbiome harbors a variety of different bacteria and fungi, keeping a fine balance between commensal and pathogenic microorganisms [1,2]. This balance is critical for oral health, especially during wound healing around dental implants. Patients with a history of periodontitis often develop peri-implant mucositis followed by peri-implantitis [3,4]. These infectious diseases are caused by oral pathogens invading the interface between gingival soft tissue and the implant [5,6].

Oral biofilms are characterized by a rich community of diverse microbes. While most studies on oral microbiomes focus on bacteria, other microbes such as fungi are also present and may play important roles in multispecies biofilms [7–9]. In oral model systems, *C. albicans* has been shown to act as bridge for the adhesion of various bacteria such as *F. nucleatum*, *S. mutans*, *S. gordonii*, and *P. gingivalis* [8,10]. Also in clinical studies, this synergism between pathogenic bacteria and *C. albicans* has been associated with periodontal diseases [11–13]. To prevent and treat oral infections, antibiotics are routinely used adjunctive to mechanical removal of microorganism accumulated in plaque [14,15]. However, with the global rise of microbial resistance [16], more and more periodontal disease related bacteria and fungi have become insusceptible to common antimicrobial agents [17–19].

Today, patients who lose teeth due to oral infections typically receive dental implants to restore masticatory function and aesthetics [20]. However, these patients are also considered to be at high risk of reoccurring infections. Thus, strategies have to be developed to prevent microbial colonization of implant surfaces. One strategy is to directly modify the implant surface to reduce adhesion or growth of microbes around the implant.

Plant polyphenols are an emerging class of antimicrobial molecules with the ability to form coatings on many materials, including titanium

* Corresponding author.
E-mail address: hanna.tiainen@odont.uio.no (H. Tiainen).

https://doi.org/10.1016/j.colsurfb.2022.112813
Received 21 July 2022; Received in revised form 22 August 2022; Accepted 26 August 2022
Available online 29 August 2022

[21]. These molecules possess ortho-di- or tri-hydroxyphenyl groups, which interact with proteins and enzymes, and chelate metal ions [22]. Based on these interactions with biomolecules, polyphenols have shown to possess broad spectrum antibacterial and antifungal properties by cell wall and cell membrane interactions, inhibition of enzymes and complexation of ions vital for regular cell metabolism [23,24]. Recent studies have demonstrated that these inhibitory effects also reduce the growth and biofilm formation of bacteria and fungi related to oral infections [25–28]. Particularly the virulence of *C. albicans* is affected by phenolic compounds via suppression of quorum sensing and hyphae formation of the fungal cells [27,29]. Thereby, the associated bacterial adhesion to cell wall proteins found on *C. albicans* hyphae could be reduced [30].

Since polyphenolic molecules are able to form coatings on almost any substrate [21], modified implant surfaces may enable local control of microbial colonization. Such approaches were investigated for pyrogallol and curcumin modified surfaces and showed a reduction of *C. albicans* adhesion [31,32]. However, in vivo, the implant surface will be covered by a salivary protein layer. Thereby, the antimicrobial properties of polyphenolic coatings may be masked, which reduces their efficacy [33].

Therefore, we investigated the adsorption of salivary proteins and the subsequent adhesion and biofilm formation of *C. albicans* on titanium surfaces coated with the polyphenols tannic acid (TA) and pyrogallol (PG). TA and PG possess ortho-di- and tri-hydroxyphenyl groups and are able to form coatings beyond mere monolayers [34,35]. We hypothesized that microbial growth may be modulated through a change in surface chemistry and the release of molecules from the surface. The latter was addressed to investigate whether TA and PG nanocoatings allow the release of a growth inhibitory concentration of polyphenolic molecules to provide substantial antimicrobial properties. Subsequently, the fungal adhesion was investigated to evaluate whether TA and PG modified surfaces can modulate the colonization of *C. albicans* and how the salivary pellicle affects the adhesion of yeast cells on modified surfaces.

2. Materials and methods

2.1. Chemicals

Tannic acid (TA, LOT#MKBN9606V), pyrogallol (PG), HEPES (Bio-Performance, ≥99.5%), and sodium metasilicate pentahydrate (Si_{aq}, ≥95%) were purchased from Sigma Aldrich. Beetleglow reagent was prepared by mixing 36 parts luciferin solution (2 mM luciferin, 25 mM glycilglycine) with 64 parts luciferase buffer (25 mM glycilglycine, 15 mM K_2HPO_4, 15 mM $MgSO_4$, 4 mM EGTA, 2 mM ATP, 1% dodecyl-β-maltoside) [36].

2.2. Coating formation

Polished titanium (Ti) coins (∅6 mm) were coated with tannic acid (TA) and pyrogallol (PG) for 24 h under sterile condition by placing 3 coins in 15 ml vials with 10 ml of polyphenolic solution and gently agitating the vials at 30 rpm. 1 mg/ml TA was dissolved in in 100 mM HEPES containing 600 mM NaCl, 80 μM Si_{aq} at pH = 6.8 or pH = 7.8. 1 mg/ml PG was dissolved in 100 mM HEPES containing 100 mM $MgCl_2$ at pH = 7.0. The obtained coated surfaces are referred to as TA 68, TA 78, and PG 70.

2.3. Surface characterization

Topography. The roughness of the used surfaces was assessed before and after the coating process at different length scales by using profilometry and atomic force microscopy (AFM). For profilometry (S neox, SensoFar), a 20 × objective (field of view: 845 ×707 μm) was used to scan 5 samples in interferometric mode. The raw data was processed by a 5 mm cut-off filter and separating the waviness from the roughness. For AFM analysis (MFP 3D, Asylum Research), 5 samples were scanned using an AC240TS cantilever in contact mode at a scan angle of 90°, a scan rate of 0.75 Hz, and a scan-area of 20 μm × 20 μm.

Wettability. Surface energy (γ_S) was calculated from linear regression of a series of contact angles (θ) using deionized water, diiodomethane, formamide, and glycerol according to the OWRK-model stated in the supplementary information [37]. Contact angles were determined by drop shape analysis (OCA-20, Dataphysics). For each surface, averages of 10 sessile drops were analyzed using the Young-Laplace fit. Silicon wafers were used as substrates for coatings to minimize fluctuation in the surface topography affecting the contact angle.

Surface charge. The surface zeta potential (ζ) of Ti surfaces, Si wafers, and coated Si wafers was determined in 5 mM saline water at a conductivity of 0.5 mS/cm using a Nano ZS Zetasizer (Malvern Panalytical) and negatively charged COOH terminated polystyrene tracer particles (100 nm, 250 μg/ml, Micromod Partikeltechnologie GmbH). The applied voltage was set to 10 V. The pH was adjusted with HCl and NaOH.

Oxidation state. The surface chemistry of the coatings was assessed by their ability to reduce $AgNO_3$ to elemental Ag. Coated glass slides were placed into 100 mM $AgNO_3$ (≥99.9%, Sigma Aldrich) for 24 h and inspected by SEM/EDS (Hitachi TM3030) for Ag deposition. Additionally, the coatings were analyzed using Fourier-transform infrared (FTIR) spectroscopy. After subtraction of the background and baseline correction, the fingerprint region from 2000 cm^{-1} to 1400 cm^{-1} was analyzed.

Saliva collection. Stimulated saliva was collected from 6 healthy non-smoking donors for 20 min while chewing on Parafilm. Donors had no food intake 2 h prior to the collection and were only allowed to drink water. Saliva was collected in sterile ice-chilled tubes and then centrifuged at 7500 g at 4 °C for 10 min. The supernatant was pooled, aliquoted, and stored at − 80 °C. According to the Norwegian Research Ethics Committee, no ethical approval for the use of this anonymized biological material is required.

Low molecular weight components were separated by dialysis (MWCO 14 kDa) against water containing 1 mM EDTA at 4 °C and subsequently freeze-dried. The yield was determined by UV-adsorption measurement (NanoDrop One, ThermoFisher Scientific) at λ = 280 nm where one absorbance unit equals to a protein concentration of 1 mg/ml.

Protein adsorption. Stimulated saliva was diluted to 25% (v/v) with PBS, mucin and lysozyme were dissolved in PBS at 200 μg/ml, and LMW salivary proteins were diluted in PBS to 500 μg/ml. The adsorption was studied using a quartz crystal microbalance with dissipation monitoring (QCM-D; QSense E4, Biolin Scientific). After equilibration of the Ti sensors (QSX310, f_0 = 4.95 MHz) in PBS, the protein solution was flown for 5 min at 100 μl/min. The flow-speed was then reduced to 10 μl/min. After the adsorption of the proteins, the layer was rinsed with PBS at 100 μl/min. Experiments were performed at least three times recording the fundamental frequency and the 3rd, 5th, 7th, 9th, and 11th harmonic (f_n). For clarity only changes in frequency (ΔF) and dissipation (ΔD) for f_n = 3, 5, and 7 are shown. Viscoelastic properties and adsorbed mass were modeled using DFind (v. 1.2.7) using the *SmartFit* function with the frequency dependent viscosity (η) and elastic modulus (μ) enabled depending on the quality of the fit. The loss tangent (G''/G') was calculated from the fitted parameters according to following equation.

$$G = G' + iG'' = \mu + i2\pi\eta f_0$$

2.4. C. albicans culture

BWP17 wild-type and a luciferase expressing ACT1RH strain of *C. albicans* were pre-cultured on YPD agar plates (50 g/l YPD, 25 g/l agar) over night at 30 °C [36]. A culture stock solution was prepared before the experiment by inoculating selected colonies in YPD broth

medium (10 g/l yeast extract, 20 g/l peptone, 1% glucose) and incubating the suspension over night at 37 °C in 5% CO_2 atmosphere.

Biofilm formation.

Candida stock solutions were diluted to $OD_{600} = 0.3$ and coated Ti coins (n = 3) were incubated with 1 ml cell suspension at 37 °C (Fig. S1). After 6 h, 24 h and 48 h, the surfaces were carefully washed with PBS to remove unbound fungal cells and then transferred to 1 ml PBS. The biofilm was dispersed by tip sonication (Vibra-Cell, Sonics & Materials Inc.) at 5 W output power for 20 s. Three 100 µl aliquots per sample were taken from the dispersed biofilm solution and from the initial incubating solution to assess the number of bacteria in biofilms and planktonic bacteria, respectively. The biofilm samples were lysed immediately in liquid nitrogen, while the planktonic samples were first washed with PBS by centrifugation for 6 min at 5000 g at 4 °C. After lysis, 100 µl Beetleglow reagent was added per 100 µl sample and the maximal luminescence was analyzed using a luminescence plate reader (Synergy HT, BioTek) for 15 min at intervals of 5 min with shaking before each readout. In total 3 individual samples were analyzed with 3 technical replicates each and 3 luminescence reads.

To support luminescence readings, colony-forming units (CFUs) were counted after incubating two 20 µl drops per sample on YPD agar plates for 48 h at 37 °C. The remaining biofilm cell suspension was used to quantify total biomass by weight. Therefore, 400 µl aliquots were diluted with 1.2 ml EtOH and dried at 60 °C under reduced pressure for 1 h.

Biofilms were visually analyzed by scanning electron microscopy (Hitachi SEM TM3030). Samples were fixed in PBS containing 2% glutaraldehyde, dried in a series of 50%, 70%, 90%, 95%, and 100% EtOH for 10 min each, and subsequently sputter coated with gold.

2.5. Fungal adhesion

C. albicans HWP17 stock solutions were washed twice with PBS (6 min, 5000 g, 4 °C) and resuspended in PBS at $OD_{600} = 0.04$. Subsequently, the cells were stained with 1 µl/ml of 3.34 mM SYTO 9 dye (BacLight, ThermoFisher Scientific) for 30 min in the dark at room temperature.

Adhesion of *C. albicans* was investigated using 0.4 mm channel slides (IBIDI, Cat.No:80178) mounted on coated glass substrates. A flowrate of 100 µl/min was chosen to induce laminar flow with a shear stress of 0.1 dyn/cm^2. Cells were allowed to adhere for 30 min. Before quantification, the chamber was rinsed with PBS. For the study of fungal adhesion on salivary pellicles, saliva was allowed to adsorb for 30 min prior to flowing the fungal cell suspension. Five images per sample were acquired using a fluorescence microscope (480/535 nm, Nikon Eclipse 90i) equipped with a 10 × objective. All experiments were repeated on four individual surfaces (n = 4).

Polyphenolic layers were dissolved by flushing the channel slides with acidic (pH ≈ 4) or alkaline (pH > 9) PBS after the adsorption experiments were conducted.

2.6. Statistical analysis

Statistical significances ($p < 0.05$) were tested using ANOVA (multcomp library) in R (Rstudio 2022.02.1) after verification of sample homogeneity and normality.

3. Results

3.1. Surface characterization

The topographic characterization using profilometry showed a roughness of $S_Q^{prof} = 12$ nm for polished Ti coins. The roughness of the Si substrate was 6 nm and TA, and PG coatings were only slightly rougher than the Si substrate (Table 1). Assessment by AFM revealed an increased roughness (S_Q^{AFM}) of the coatings compared to Ti surfaces. The increased roughness was caused by the incorporation of precipitated TA and PG particles in the surface during the coating process (Fig. S2).

Both TA and PG coatings were of hydrophilic nature, with water contact angles (WCA) below 32° (Table 1). This is further reflected in a high surface energy, which approached values of the UV-ozone treated Si wafers. In comparison to Ti, TA and PG coatings have a significantly higher polar component and are more negatively charged (Table 1, Fig. S3).

Two different TA coatings were prepared with the hypothesis that under reduced pH, the coating remains in a non-oxidized state. FTIR analysis of the surface confirmed this assumption and showed a spectrum for TA 68 coatings similar to pristine TA (Fig. S4). In contrast, TA 78 and PG 70 coatings showed oxidation of the coating. This difference in surface chemistry was further manifested in the reduction of $AgNO_3$. TA 68 showed a higher reduction of $AgNO_3$ compared to TA 78 and caused the formation of elemental Ag particles within minutes after immersion in $AgNO_3$ solution (Fig. S4). Although PG 70 showed oxidation in FTIR, it effectively reduced Ag^+ cations and showed a continuous Ag coating on the surface during 24 h immersion in $AgNO_3$.

3.2. Salivary pellicle formation

Both TA 78 and TA 68 coated surfaces facilitated the adsorption of salivary proteins. QCM-D experiments show a higher mass of the adsorbed protein layer on the TA coatings compared to Ti surfaces (Fig. 1a). PG 70 coatings resulted in almost equal amount of adsorbed salivary proteins compared to Ti, despite their different surface chemistry (Table 1).

In addition to changes in the equilibrium mass, the kinetics of saliva adsorption was obtained. The adsorption of salivary proteins on polyphenolic coatings is defined by a rapid initial adsorption, followed by minor changes in frequency and dissipation over time (Fig. S5). In contrast, on Ti surfaces a gradual formation of the pellicle was observed (Fig. S5). This change in pellicle structure was also visible in the visco-elastic parameters of the salivary protein film (Fig. 1b and c). On both Ti and PG coatings, a lower viscosity but higher elastic modulus was obtained compared to TA coatings. To correlate the change in viscosity and elastic modulus, the loss tangent can be calculated. This parameter visualizes a more obvious change in visco-elastic properties as shown in Fig. 1d. Both TA 68 and TA 78 coatings result in a more liquid like saliva pellicle with G''/G′ values below 1, while the protein film on Ti and PG 70 showed values greater than 1. Further, the change in protein film structure on TA coatings was corroborated by the splitting of the harmonics recorded by QCM-D during the adsorption (Fig. S5). Despite the

Table 1
Physico-chemical properties of polyphenolic coatings.

	S_Q^{prof} (nm)	S_Q^{AFM} (nm)	γ_S^P (mN/m)	γ_S^D (mN/m)	γ_S (mN/m)	WCA (°)	ζ (mV)
Ti	12.0 ± 2.6	5.3 ± 1.8	13.2	30.2	43.4	64	-28.4 ± 4.5
Si	6.2 ± 0.7	1.0 ± 0.1	41.2	24.1	65.3	24	-44.0 ± 1.8
TA 68	7.6 ± 1.2	30.8 ± 1.8	34.5	28.2	62.7	32	-59.0 ± 1.7
TA 78	7.9 ± 1.3	32.7 ± 7.2	40.4	24.4	64.8	20	-56.5 ± 5.6
PG 70	10.3 ± 2.7	21.2 ± 2.5	42.5	24.9	67.4	14	-65.3 ± 4.0

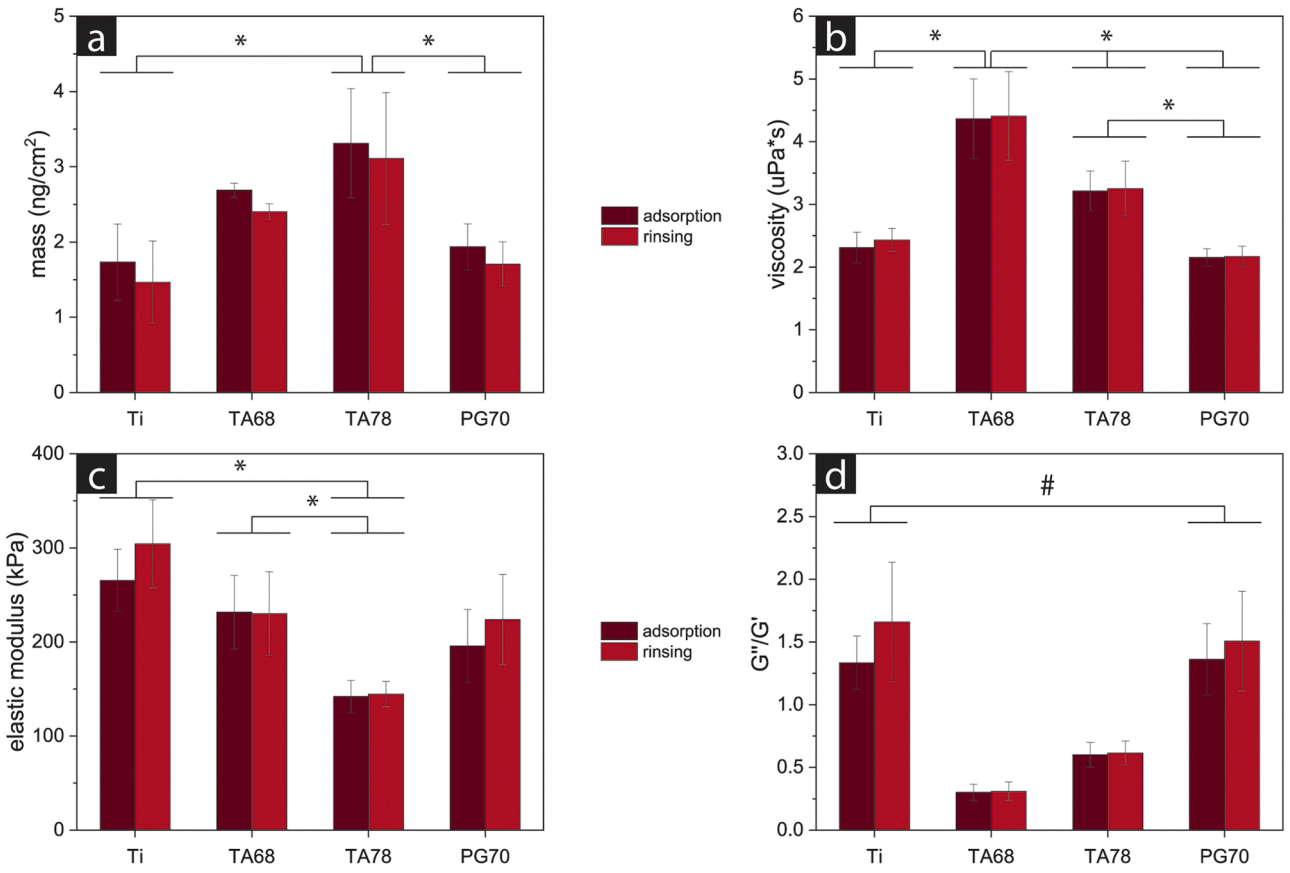

Fig. 1. Properties of salivary pellicles formed on Ti, TA 68, TA 78, and PG 70 surfaces as determined by QCM-D. (a) Mass, (b) viscosity, and (c) elastic modulus of the adsorbed protein layer after 1 h (absorption) and after a subsequent rinsing step with PBS for 30 min (rinsing). (d) Ratio of storage modulus (G'') and loss modulus (G'). The figure shows mean and standard deviation for 4 individual replicates per surface ($n_e = 4$). Statistically significant differences are marked with asterisks (*), while (#) denotes the only non-significant difference among the test groups.

different pellicle structure, all surfaces showed a similar amount of proteins desorbing from the layer upon rinsing with PBS (Fig. 1a).

3.3. Adsorption of salivary components

Ti surfaces effectively resisted mucin adsorption as shown by the low change in frequency and dissipation in Fig. 2a. The presence of polyphenolic coatings increased the adsorption of mucin with TA 78 coatings showing the largest gain in mass (Fig. S6). The protein layer further showed a highly dissipative structure on TA 78 coatings compared to TA 68 and PG 70 coatings (Fig. 2a). This higher amount of apparently loosely bound proteins on TA 78 desorbed in the subsequent rinsing step with PBS (Fig. S6 and S7).

In contrast to mucin, the adsorption of lysozyme on Ti showed a larger change in frequency and dissipation, but both proteins show linear adsorption kinetics (Fig. 2). Lysozyme showed only little desorption from Ti upon rinsing with PBS (Fig. S6). On TA and PG coatings, high initial binding was followed by linear adsorption kinetics (Fig. 2b). TA 78 surfaces bound the highest amount of lysozyme with prolonged desorption upon rinsing with PBS compared to TA 68 and PG 70 (Fig. S8). On both TA coatings, splitting overtones were observed indicating a heterogeneous layer structure (Fig. S8).

3.4. Competitive adsorption of proteins

The initial salivary pellicle formation was mimicked by the adsorption of dialyzed low molecular weight (LMW) components. After the adsorption of the LMW proteins on Ti, the subsequent adsorption of mucin reached similar change in frequency and dissipation compared to the bare Ti surface (Fig. 3). More importantly, the mucin adsorption on polyphenolic coatings was reduced after the adsorption of LMW proteins. The adsorbed mass showed equal levels for Ti surfaces and all three polyphenolic coatings.

3.5. Fungal biofilm formation

The presence of a polyphenol coating did not appear to reduce the growth rate of *C. albicans* in our experimental model. While the luminescence readings of cells in biofilms at different time points shown in Fig. 4a were close to background levels, the higher number of planktonic cells in the supernatant allowed a more reliable quantification but showed no reduction of fungal growth in the presence of polyphenolic surfaces (Fig. 4b). However, the optical density (OD600) increased for both biofilm and planktonic samples indicating the growth of fungi during the experiment (Fig. 4c, d). The simultaneous quantification of CFUs and total biomass corroborated the luminescence and optical density data indicating no inhibition of planktonic growth and biofilm formation. (Fig. S9). SEM imaging of the biofilm showed that ACT1 and BWP17 formed a dense coverage of the Ti surface with *Candida* cells after 6 h (Fig. S10). However, less cells were found for subsequent time points. In comparison to Ti, TA 68 and TA 78 coatings showed a reduced cell count on the surface during the early phase of the biofilm formation. Thereafter, the adherent cell number slightly increased after 24 h and 48 h. PG 70 had the lowest count of adherent cells throughout the analyzed time points. In general, mostly yeast cells were observed with only few forming hyphae, which was in accordance with the culture condition [36].

Analysis of *C. albicans* ACT1RH inhibition in presence of free TA and

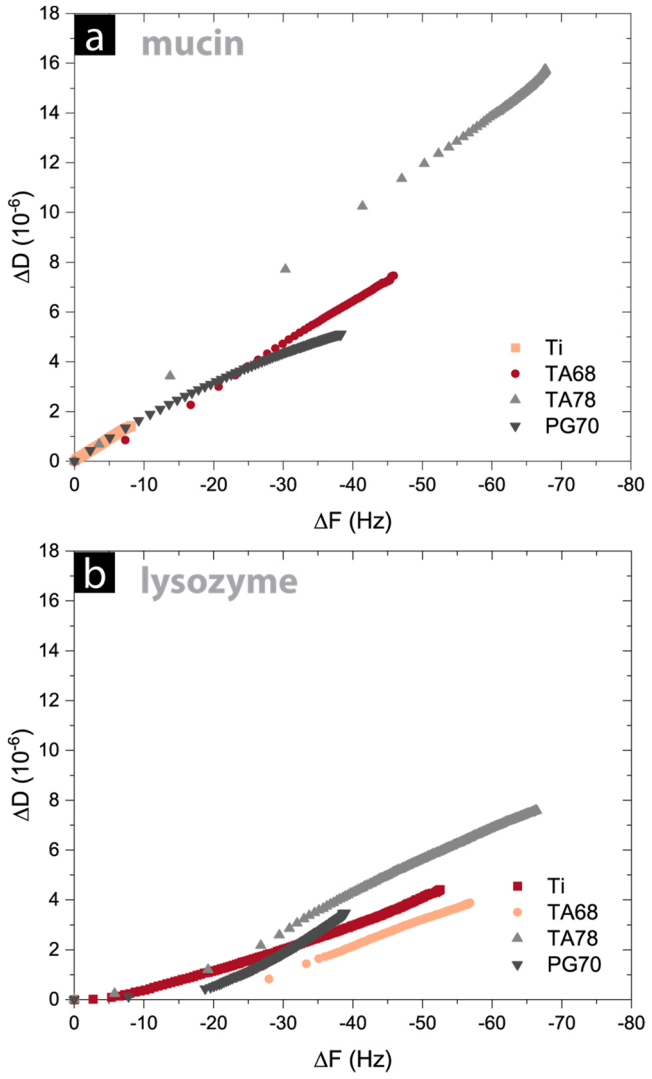

Fig. 2. (a) Mucin and (b) lysozyme adsorption under continuous flow monitored by QCM-D. Both proteins were reconstituted at 200 μg/ml in PBS at pH = 7.0. Figures show the average change in $\Delta D/\Delta F$ (f_n = 5) of four individual adsorption curves (n_e = 4) recorded for 1 h. For clarity, the error bars were omitted.

PG showed that both molecules had a dose-dependent antifungal activity (Fig. S11). Complete inhibition of planktonic *Candida* growth was not observed at concentrations ≤ 4.05 mg/ml at a seeding density of OD600 = 0.3 used in the experimental setup. The antifungal activity became more significant at 100 and 1000-fold dilution of the inoculate. The half maximal inhibitory concentrations (IC50) for 1000-fold dilution of the inoculate were found to be 57 μg/ml TA and 165 μg/ml PG.

3.6. Fungal adhesion

C. albicans adhesion was lower on polyphenolic coatings that were not pre-conditioned with saliva compared to the glass substrate (Figs. 5 and S12). During a period of 30 min cells attached on all surfaces under a flow with a shear stress of 0.1 dyn/cm^2. While flushing with PBS did not remove any cells, dissolving the polyphenolic layer caused detachment of the cells (supplementary video material).

Supplementary material related to this article can be found online at doi:10.1016/j.colsurfb.2022.112813.

After forming a salivary pellicle on the surfaces, the glass substrate showed a reduction in cell adhesion compared to the bare glass slide. Similarly, the salivary protein film formed on TA and PG coatings

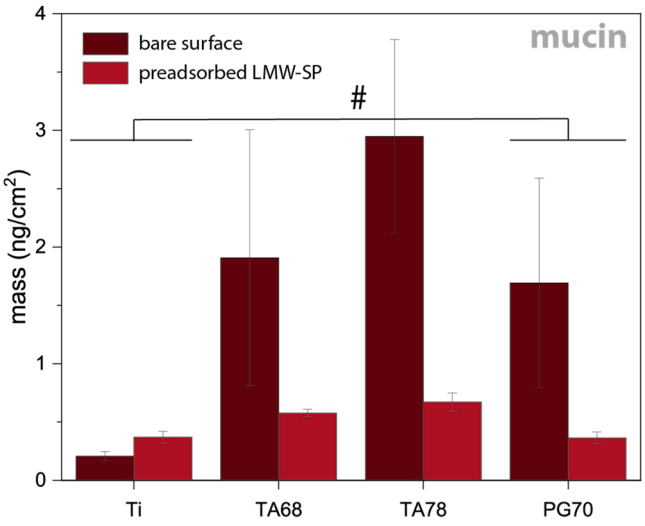

Fig. 3. Adsorption of mucin onto LMW salivary proteins (LMW-SP) compared to bare surfaces. Bars show the change in frequency and dissipation for the 5th harmonic monitored by QCM-D. The LMW protein layer was allowed to form for 2 h on the surfaces before ΔF and ΔD were offset, and mucin was adsorbed for 1 h. Results are given as mean ± SD of four individual replicates (n_e = 4). (#) denotes the only non-significant difference among the groups.

reduced the *Candida* adhesion compared to the coated surfaces. However, the number of cells on the saliva pellicle formed on polyphenolic surfaces was higher compared to the adhesion on the saliva conditioned glass surface with no polyphenolic coating.

4. Discussion

Polyphenolic molecules are an emerging class of antimicrobial molecules [24], which show antifungal properties and inhibit the growth of *C. albicans* [27,28,32,38]. With the possibility to form coatings on a multitude of surfaces, their use for antimicrobial and antibiofouling surface modifications caught scientific interest [39–41]. Due to the release of polyphenolic molecules from coated surfaces [34], we hypothesized that thicker coatings release enough active molecules to prevent the growth of *C. albicans*. However, we did not observe inhibition of *C. albicans* growth (Fig. 4). This was in part due to the small number of cells bound to the samples, which did not allow a reliable luminescent reading. However, the increase in optical density and CFUs indicated normal growth of *C. albicans* in the presence of polyphenols (Fig. 4 and S9). This indicated that the concentration of polyphenols released from the coatings was too low to inhibit growth and biofilm formation of *C. albicans* in our experimental setup. For most polyphenolic molecules, a MIC above 100 μg/ml is reported [27,32,38]. Our results on antifungal activity of free TA and PG against *C. albicans* ACT1RH (Fig. S11) agreed with these reports. For our coatings, which have a thickness between 100 nm and 200 nm [34,35], and a surface area of 104 mm^2 of the test specimen, the theoretical maximum concentration of polyphenolic molecules released into the growth medium is below 40 μg/ml. Hence the general MIC was not reached and the local concentration near the surface was not effective to inhibit the growth of *C. albicans*.

However, we observed that biofilms easily disrupted on TA and PG coatings. *Candida* cells appeared to not adhere well to the coated surfaces, as observed in the SEM analysis (Fig. S10). Indeed, such anti-adhesive properties of polyphenolic coatings have been observed for PG and curcumin [31]. Hence, this mechanism would open a second route to prevent fungal colonization of implant surfaces without selective pressure of antibiotics.

To tailor the adhesion of fungal cells, an understanding of the surface

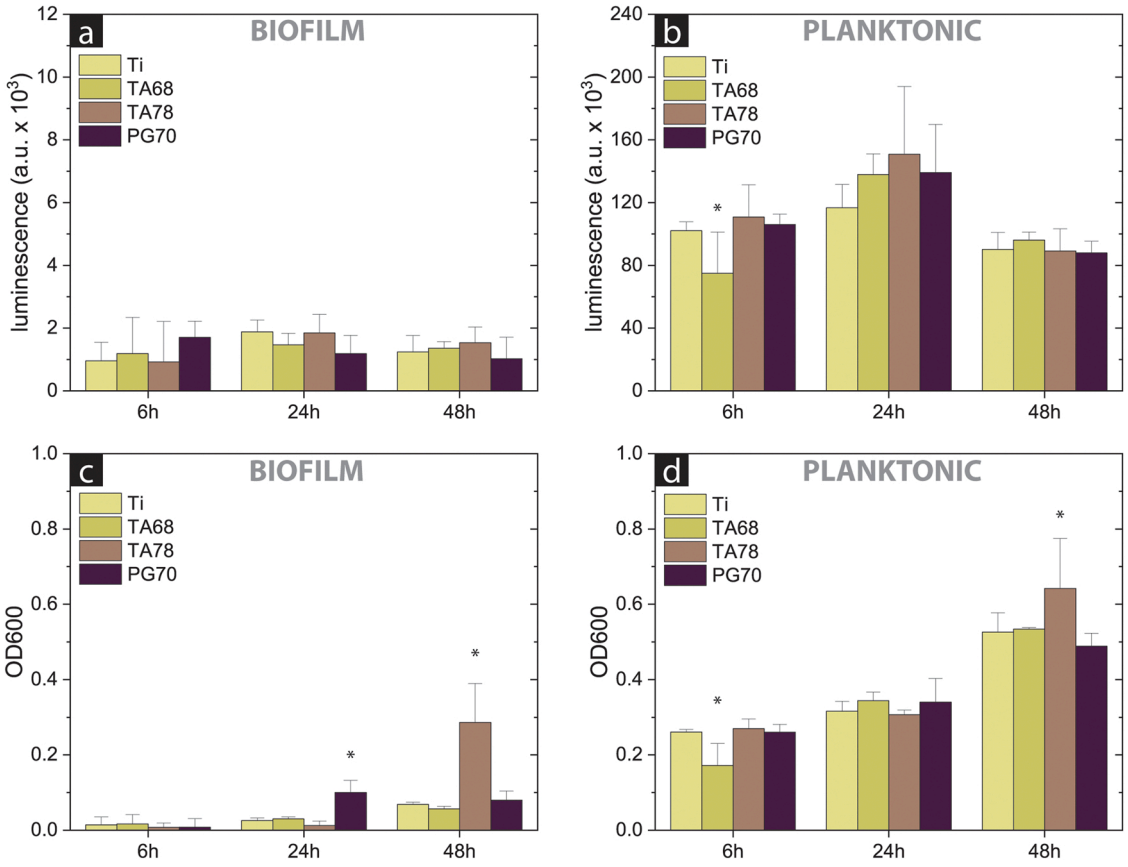

Fig. 4. *C. albicans* ACT1 growth in a biofilm model using Ti and polyphenol coated Ti surfaces. Cells in the resuspended biofilm and in the planktonic fractions were quantified using luminescence (a, b). Additionally, optical density was determined at λ = 600 nm (c, d). Values are given as mean ± SD of three individual samples with each three technical replicates (n_e = 9). Statistically significant differences are marked with asterisks (*).

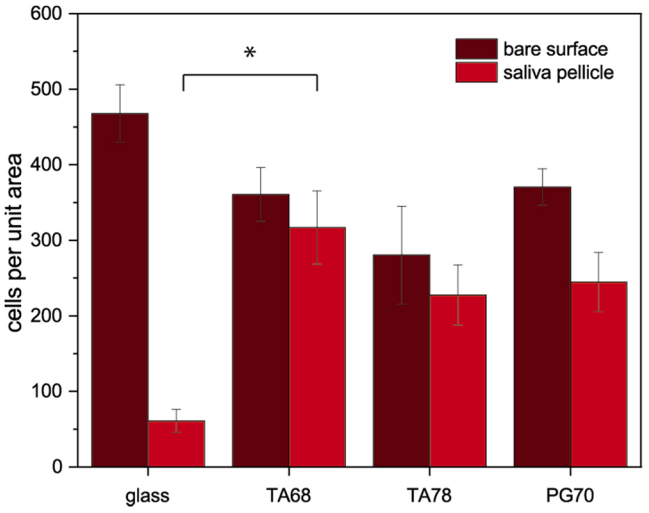

Fig. 5. Adhesion of *C. albicans* on polyphenolic coatings pre-conditioned or not with salivary pellicles. Cells were allowed to attach under constant flow for 30 min. Experiments were performed on four individual surfaces (n_e = 4). Values are represented as mean ± SD. Statistically significant differences are marked with asterisks (*).

chemistry and topography is important. Properties such as wettability, hydrophobicity, charge, and roughness are known factors influencing microbial adhesion [42]. *C. albicans* attachment is typically favored on hydrophobic surfaces, whereas negatively charged surfaces are less prone to adhesion due to electrostatic repulsion between the material surface and the negatively charged cell wall [43]. Similar to carboxylic acid modified surfaces, which reduce the adhesion of *C. albicans* [44], our coatings present hydrophilic and negatively charged properties (Table 1). However, our results showed no reduction of the adhesion of *Candida* cells (Fig. 5). This is in agreement with a study on TA-based metal phenolic networks, which presented no decrease in microbial adhesion [45]. Our previous studies also support the observation that TA and PG coatings are not able to prevent bacterial adhesion [46]. This could be due to a chemical change of the coating in the culture media, or the specific chemistry of these molecules in contrast to other hydrophilic and negatively charged surfaces.

In addition to microbial cell adhesion on bare polyphenolic coatings, we studied whether salivary protein layers influence the subsequent adhesion of *C. albicans*. Since trans-mucosal dental implants face the immediate challenge of protein adsorption from the oral cavity, the surface characteristics the microorganisms experience are dominated by the properties of the formed conditioning film. It has been shown that whole saliva, particularly mucin, facilitates the adhesion of C. albicans [47]. In combination with a strong interaction of polyphenolic molecules with proteins [48], these coatings may even facilitate fungal adhesion after the formation of a salivary pellicle. Indeed, both TA-coated surfaces showed the formation of a thicker and more liquid-like salivary pellicle (Fig. 1). The observed difference in protein adsorption can be explained by the change in surface chemistry driving the changes in the structural composition of salivary pellicles [49]. Particularly surface charge and polarity affect the adsorption and viscoelastic properties of the protein film on different surfaces [49,50]. Negatively charged hydrophilic surfaces, such as Ti, are commonly less prone to protein adsorption compared to hydrophobic surfaces [51]. However, the adsorption of all studied proteins on the hydrophilic

polyphenolic surfaces was larger than for Ti surfaces (Figs. 1 and 2). This observation agrees with previous studies showing high binding affinity and immobilization of proteins on polyphenolic surfaces [52,53]. Increased protein adsorption can be caused by altered surface topography, but we consider the slight increase in the nanometer range negligible in relation to the obtained QCM-D signal.

Further investigation of the adsorption of salivary components revealed a high affinity of TA to mucins. This specific binding affinity of proteins is important when studying complex proteinaceous solutions such as saliva. In these systems, the adsorption of individual components is governed by the Vroman effect [54]. This effect describes the initial adsorption of LMW proteins followed by their replacement by larger proteins with higher affinity. In the oral cavity, mucins are ubiquitous high molecular weight proteins and represent the main component *C. albicans* experiences upon invading mucosal tissues [55]. Due to the glycosylation of mucin presenting hydrophobic moieties at the C- and N-terminus, the protein adopts a flat conformation on Ti surfaces [56,57]. In comparison, the high affinity of the cysteine rich domains to polyphenolic surfaces can explain the strong interaction with our coatings [58]. An altered conformation of mucin on TA and PG coatings may then expose different domains of the protein, similarly to gold and hydrophobic surfaces [59,60]. Since *C. albicans* preferably binds to a 188 kDa C-terminal glycopeptide in intestinal mucins [61], the adsorption of mucin can play a critical role for *Candida* adhesion. However, the initial adsorption of low molecular weight proteins to the surface dictates the later mucin adsorption. During sequential protein adsorption, it has been found that the adsorption of the second protein is lower compared to the adsorption of the same protein on a clean surface [62]. In accordance with this observation, LMW proteins reduced the adsorption of mucin on the TA and PG modified surfaces (Fig. 3). In vivo, the adsorption of components still occurs parallel and TA surfaces may foster the adsorption of mucins.

In addition to mucin adsorption, we studied the adsorption of lysozyme on polyphenolic surfaces. Lysozyme is able to cleave the peptidoglycan structure of microbial cell walls [63], and could potentially reduce microbial colonization. In comparison to mucin layers, lysozyme displayed a continuous adsorption profile (Fig. 2), due to the electrostatic interactions of the negatively charged surface and the positively charged lysozyme (pI = 11) [64–66]. It is vital that after adsorption the enzymatic activity of lysozyme is maintained. However, dissolved TA and adsorption to hydrophobic surfaces can inactivate the enzyme [67,68]. We expect that hydrophilic polyphenolic surfaces may not inflict with the functional properties, as a study using hydrophilic stainless steel surface suggests [69]. This hypothesis is supported by a study of the antimicrobial activity of TA and lysozyme multilayers against *S. aureus*, showing retained activity of the enzyme [70].

Since our studies with salivary proteins indicated a change in structure and conformation of the pellicle on TA and PG coatings, we investigated whether this affects the adhesion of *C. albicans*. While we found a similar number of adherent cells on glass and polyphenolic layers, the saliva film formed on TA and PG facilitated the adhesion in contrast to the glass substrate (Fig. 5). This confirmed the impact of our coatings on the structure of saliva films. It is, however, unclear why the protein layer on glass showed fewer adherent cells. Additionally, we saw that adherent cells on the glass surface and on the coating could not be detached by rinsing with PBS. However, the polyphenolic layer can be dissolved in either acidic or alkaline environment [71]. Thereby, it is possible to release attached cells from the modified surfaces (supplementary video material) and the coatings could be used as a pH sensitive sacrificial layer.

Finally, we would like to highlight the conflict of the required high concentration of polyphenols for an antimicrobial effect with the impact on human cells. Our investigation showed IC50 concentrations of 57 μg/ml and 165 μg/ml for TA and PG for *C. albicans* inoculated at OD $= 3 \times 10^{-4}$ (Fig. S11). For these concentrations, we have previously seen detrimental effects on cell viability and cell morphology of human gingival fibroblasts [71].

5. Conclusion

Polyphenolic surface modifications were not able to prevent *C. albicans* colonization through reduction of growth. The release of active molecules from the coatings was below the MIC for *C. albicans* and an increase of the concentration may negatively affect human cell adhesion towards modified implant surfaces.

Further, adhesion of yeast cells onto modified surfaces was not inhibited under flow, despite the hydrophilic surface properties of TA and PG coatings. However, a potential antibiofilm effect was observed by the pH-dependent disassembly of the polyphenolic layer, which caused biofilms to detach from the surface.

TA and PG coatings have a high affinity for protein adsorption, which influenced the competitive binding of proteins from saliva. This resulted in the formation of a protein film that allowed *C. albicans* adhesion in contrast to a salivary pellicle formed on glass.

In conclusion, simple polyphenolic surface modifications may not have a long-term antimicrobial effect and further efforts are required to create polyphenolic coatings that balance tissue integration with prevention of microbial colonization of implant surfaces.

Funding sources

This work was financially supported by the Research Council of Norway, grant number 302590.

CRediT authorship contribution statement

Florian Weber: Methodology, Investigation, Formal analysis, Writing – original draft, Writing – review & editing. **Louise Morais Dornelas-Figueira:** Investigation, Methodology. **Nora Hafiane:** Investigation. **Daria Zaytseva-Zotova:** Investigation, Writing – review & editing. **Alejandro Barrantes:** Writing – review & editing. **Fernanda Cristina Petersen:** Writing – review & editing. **Hanna Tiainen:** Conceptualization, Supervision, Writing – review & editing.

Declaration of Competing Interest

The authors declare that they have no known competing financial interests or personal relationships that could have appeared to influence the work reported in this paper.

Data availability

Data will be made available on request.

Acknowledgements

We thank Lasse Van Wijlick and Joachim Ernst for providing us with the Candida strains used in the study.

Appendix A. Supporting information

Supplementary data associated with this article can be found in the online version at doi:10.1016/j.colsurfb.2022.112813.

References

[1] R. Pokrowiecki, A. Mielczarek, T. Zaręba, S. Tyski, Oral microbiome and peri-implant diseases: where are we now? Ther. Clin. Risk Manag 13 (2017) 1529–1542.

[2] B. Sampaio-Maia, I.M. Caldas, M.L. Pereira, D. Pérez-Mongiovi, R. Araujo, The oral microbiome in health and its implication in oral and systemic diseases, Adv. Appl. Microbiol 97 (2016) 171–210.

[3] I.K. Karoussis, G.E. Salvi, L.J.A. Heitz-Mayfield, U. Brägger, C.H.F. Hämmerle, N. P. Lang, Long-term implant prognosis in patients with and without a history of chronic periodontitis: a 10-year prospective cohort study of the ITI® Dental Implant System, Clin. Oral Implants Res. 14 (3) (2003) 329–339.

[4] J. Lindhe, J. Meyle, Peri-implant diseases: consensus report of the sixth European workshop on periodontology, J. Clin. Periodontol. 35 (2008) 282–285.

[5] J.E. Botero, A.M. González, R.A. Mercado, G. Olave, A. Contreras, Subgingival microbiota in peri-implant mucosa lesions and adjacent teeth in partially edentulous patients, J. Periodontol. 76 (9) (2005) 1490–1495.

[6] I. Sanz-Martin, J. Doolittle-Hall, R.P. Teles, M. Patel, G.N. Belibasakis, C.H. F. Hämmerle, R.E. Jung, F.R.F. Teles, Exploring the microbiome of healthy and diseased peri-implant sites using Illumina sequencing, J. Clin. Periodontol. 44 (12) (2017) 1274–1284.

[7] W.G. Wade, The oral microbiome in health and disease, Pharmacol. Res. 69 (1) (2013) 137–143.

[8] B.P. Krom, S. Kidwai, J.M. Ten Cate, *Candida* and other fungal species: forgotten players of healthy oral microbiota, J. Dent. Res 93 (5) (2014) 445–451.

[9] J.L. Baker, B. Bor, M. Agnello, W. Shi, X. He, Ecology of the oral microbiome: beyond bacteria, Trends Microbiol. 25 (5) (2017) 362–374.

[10] R. Tamai, M. Sugamata, Y. Kiyoura, *Candida albicans* enhances invasion of human gingival epithelial cells and gingival fibroblasts by Porphyromonas gingivalis, Microb. Pathog. 51 (4) (2011) 250–254.

[11] J. Slots, T.E. Rams, M.A. Listgarten, Yeasts, enteric rods and pseudomonads in the subgingival flora of severe adult periodontitis, Oral Microbiol. Immunol. 3 (2) (1988) 47–52.

[12] A. Canabarro, C. Valle, M.R. Farias, F.B. Santos, M. Lazera, B. Wanke, Association of subgingival colonization of *Candida albicans* and other yeasts with severity of chronic periodontitis, J. Periodontal Res. 48 (4) (2013) 428–432.

[13] J. De-La-Torre, G. Quindós, C. Marcos-Arias, X. Marichalar-Mendia, M.L. Gainza, E. Eraso, A. Acha-Sagredo, J.M. Aguirre-Urizar, Oral *Candida* colonization in patients with chronic periodontitis. Is there any relationship? Rev. Iberoam. De. Micol. 35 (3) (2018) 134–139.

[14] J. Slots, M. Ting, Systemic antibiotics in the treatment of periodontal disease, Periodontology 2000 28 (1) (2002) 106–176.

[15] M. Esposito, M.G. Grusovin, H.V. Worthington, Interventions for replacing missing teeth: antibiotics at dental implant placement to prevent complications, Cochrane Database Syst. Rev. (7) (2013).

[16] O. World Health, Antimicrobial Resistance: Global Report on Surveillance, World Health Organization, 2014.

[17] M. Enersen, M. Hultin, E. Kønønen, A. Havemose Poulsen, R. Simm, Antibiotics in the treatment of periodontal and peri-implant infections, Nor. Tannlege Tid. 129 (2019) 224–235.

[18] M. Haque, M. Sartelli, S.Z. Haque, Dental infection and resistance-global health consequences, Dent. J. 7 (1) (2019) 22.

[19] S.P. Hawser, L.J. Douglas, Resistance of *Candida albicans* biofilms to antifungal agents in vitro, Antimicrob. Agents Chemother. 39 (9) (1995) 2128–2131.

[20] Rebmann, B.H., Verena, Leonhard, Elisabeth Atlas Dental, 2019.

[21] D.G. Barrett, T.S. Sileika, P.B. Messersmith, Molecular diversity in phenolic and polyphenolic precursors of tannin-inspired nanocoatings, Chem. Commun. 50 (55) (2014) 7265–7268.

[22] S. Quideau, D. Deffieux, C. Douat-Casassus, L. Pouységu, Plant polyphenols: chemical properties, biological activities, and synthesis, Angew. Chem. Int. Ed. 50 (3) (2011) 586–621.

[23] M.M. Cowan, Plant products as antimicrobial agents, Clin. Microbiol. Rev. 12 (4) (1999) 564.

[24] M. Daglia, Polyphenols as antimicrobial agents, Curr. Opin. Biotechnol. 23 (2) (2012) 174–181.

[25] E.M. Varoni, G. Lodi, A. Sardella, A. Carrassi, M. Iriti, Plant polyphenols and oral health: old phytochemicals for new fields, Curr. Med. Chem. 19 (11) (2012) 1706–1720.

[26] K. Bunte, A. Hensel, T. Beikler, Polyphenols in the prevention and treatment of periodontal disease: a systematic review of in vivo, *ex vivo* and in vitro studies, Fitoterapia 132 (2019) 30–39.

[27] G.R. Teodoro, K. Ellepola, C.J. Seneviratne, C.Y. Koga-Ito, Potential use of phenolic acids as Anti-*Candida* agents: a review, Front. Microbiol. 6 (2015) 1420.

[28] D. Seleem, V. Pardi, R.M. Murata, Review of flavonoids: a diverse group of natural compounds with anti-*Candida albicans* activity in vitro, Arch. Oral Biol. 76 (2017) 76–83.

[29] N. Martins, L. Barros, M. Henriques, S. Silva, I.C.F.R. Ferreira, Activity of phenolic compounds from plant origin against *Candida* species, Ind. Crops Prod. 74 (2015) 648–670.

[30] M.E. Shirtliff, B.M. Peters, M.A. Jabra-Rizk, Cross-kingdom interactions: *Candida albicans* and bacteria, FEMS Microbiol. Lett. 299 (1) (2009) 1–8.

[31] H. Alalwan, R. Rajendran, D.F. Lappin, E. Combet, M. Shahzad, D. Robertson, C. J. Nile, C. Williams, G. Ramage, The anti-adhesive effect of curcumin on *Candida albicans* biofilms on denture materials, Front. Microbiol. 8 (2017) 659.

[32] M. Shahzad, L. Sherry, R. Rajendran, C.A. Edwards, E. Combet, G. Ramage, Utilising polyphenols for the clinical management of *Candida albicans* biofilms, Int. J. Antimicrob. Agents 44 (3) (2014) 269–273.

[33] Y.W. Cavalcanti, M. Wilson, M. Lewis, D. Williams, P.M. Senna, A.A. Del-Bel-Cury, W.J. d Silva, Salivary pellicles equalise surfaces' charges and modulate the virulence of *Candida albicans* biofilm, Arch. Oral. Biol. 66 (2016) 129–140.

[34] S. Geißler, A. Barrantes, P. Tengvall, P.B. Messersmith, H. Tiainen, Deposition kinetics of bioinspired phenolic coatings on titanium surfaces, Langmuir 32 (32) (2016) 8050–8060.

[35] F. Weber, W.-C. Liao, A. Barrantes, M. Edén, H. Tiainen, Silicate-phenolic networks: coordination mediated deposition of bioinspired tannic acid coatings, Chem. Eur. J. 25 (2019) 9870–9874.

[36] M. Kapitan, I. Eichhof, Q. Lagadec, J.F. Ernst, Click beetle luciferases as dual reporters of gene expression in *Candida albicans*, Microbiology 162 (8) (2016) 1310–1320.

[37] D.K. Owens, R.C. Wendt, Estimation of the surface free energy of polymers, J. Appl. Polym. Sci. 13 (8) (1969) 1741–1747.

[38] N.A. Evensen, P.C. Braun, The effects of tea polyphenols on *Candida albicans*: inhibition of biofilm formation and proteasome inactivation, Can. J. Microbiol. 55 (9) (2009) 1033–1039.

[39] F. Reitzer, M. Allais, V. Ball, F. Meyer, Polyphenols at interfaces, Adv. Colloid Interface Sci. 257 (2018) 31–41.

[40] H.A. Lee, Y. Ma, F. Zhou, S. Hong, H. Lee, Material-Independent surface chemistry beyond polydopamine coating, Acc. Chem. Res. 52 (3) (2019) 704–713.

[41] E. Kurzbaum, L. Iliasafov, L. Kolik, J. Starosvetsky, D. Bilanovic, M. Butnariu, R. Armon, From the Titanic and other shipwrecks to biofilm prevention: the interesting role of polyphenol-protein complexes in biofilm inhibition, Sci. Total Environ. 658 (2019) 1098–1105.

[42] I. Francolini, C. Vuotto, A. Piozzi, G. Donelli, Antifouling and antimicrobial biomaterials: an overview, APMIS 125 (4) (2017) 392–417.

[43] S.A. Klotz, D.J. Drutz, J.E. Zajic, Factors governing adherence of *Candida* species to plastic surfaces, Infect. Immun. 50 (1) (1985) 97.

[44] S.E. Park, A.R. Periathamby, J.C. Loza, Effect of surface-charged poly(methyl methacrylate) on the adhesion of *Candida albicans*, J. Prosthodont 12 (4) (2003) 249–254.

[45] M.-P. Ko, C.-J. Huang, A versatile approach to antimicrobial coatings via metal-phenolic networks, Colloids Surf. B Biointerfaces 187 (2020), 110771.

[46] S. Geißler, M. Gomez-Florit, D. Wiedmer, A. Barrantes, F.C. Petersen, H. Tiainen, *In* vitro performance of bioinspired phenolic nanocoatings for endosseous implant applications, ACS Biomater. Sci. Eng. 5 (2019) 3340–3351.

[47] R. Bürgers, S. Hahnel, T.E. Reichert, M. Rosentritt, M. Behr, T. Gerlach, G. Handel, M. Gosau, Adhesion of *Candida albicans* to various dental implant surfaces and the influence of salivary pellicle proteins, Acta Biomater. 6 (6) (2010) 2307–2313.

[48] E. Haslam, T.H. Lilley, E. Warminski, H. Liao, Y. Cai, R. Martin, S.H. Gaffney, P. N. Goulding, G. Luck, Polyphenol complexation, in: in: Phenolic Compounds in Food and Their Effects on Health I, 506, American Chemical Society, 1992, pp. 8–50.

[49] A. Barrantes, T. Arnebrant, L. Lindh, Characteristics of saliva films adsorbed onto different dental materials studied by QCM-D, Colloids Surf. A Physicochem. Eng. Asp. 442 (2014) 56–62.

[50] F. Weber, A. Barrantes, Real-time formation of salivary films onto polymeric materials for dental applications: differences between unstimulated and stimulated saliva, Colloids Surf. B Biointerfaces 154 (2017) 203–209.

[51] H.L. Gibbins, G.E. Yakubov, G.B. Proctor, S. Wilson, G.H. Carpenter, What interactions drive the salivary mucosal pellicle formation? Colloids Surf. B Biointerfaces 120 (2014) 184–192.

[52] B.L. Tardy, J.J. Richardson, V. Nithipipat, K. Kempe, J. Guo, K.L. Cho, M.A. Rahim, H. Ejima, F. Caruso, Protein adsorption and coordination-based end-tethering of functional polymers on metal–phenolic network films, Biomacromolecules 20 (3) (2019) 1421–1428.

[53] A.M.L. Sousa, T.-D. Li, S. Varghese, P.J. Halling, K.H. Aaron Lau, Highly active protein surfaces enabled by plant-based polyphenol coatings, ACS Appl. Mater. Interfaces 10 (45) (2018) 39353–39362.

[54] L. Vroman, A.L. Adams, Findings with the recording ellipsometer suggesting rapid exchange of specific plasma proteins at liquid/solid interfaces, Surf. Sci. 16 (1969) 438–446.

[55] I. Castro, M.-J. Barrera, S. González, S. Aguilera, U. Urzúa, J. Cortés, M.-J. González, Mucins in salivary gland development, regeneration, and disease, in: S. Cha (Ed.), in: Salivary Gland Development and Regeneration, Springer International Publishing, Cham, 2017, pp. 45–71.

[56] A.M. Wu, G. Csako, A. Herp, Structure, biosynthesis, and function of salivary mucins, Mol. Cell. Biochem. 137 (1) (1994) 39–55.

[57] M. Marczynski, B.N. Balzer, K. Jiang, T.M. Lutz, T. Crouzier, O. Lieleg, Charged glycan residues critically contribute to the adsorption and lubricity of mucins, Colloids Surf. B Biointerfaces 187 (2020), 110614.

[58] S. Ito, M. Sugumaran, K. Wakamatsu, Chemical Reactivities of ortho-quinones produced in living organisms: fate of quinonoid products formed by tyrosinase and phenoloxidase action on phenols and catechols, Int. J. Mol. Sci. 21 (17) (2020) 6080.

[59] S. Oh, M. Wilcox, J.P. Pearson, S. Borrós, Optimal design for studying mucoadhesive polymers interaction with gastric mucin using a quartz crystal microbalance with dissipation (QCM-D): Comparison of two different mucin origins, Eur. J. Pharm. Biopharm. 96 (2015) 477–483.

[60] A.A. Feiler, A. Sahlholm, T. Sandberg, K.D. Caldwell, Adsorption and viscoelastic properties of fractionated mucin (BSM) and bovine serum albumin (BSA) studied with quartz crystal microbalance (QCM-D), J. Colloid Interface Sci. 315 (2) (2007) 475–481.

[61] L. de Repentigny, F. Aumont, K. Bernard, P. Belhumeur, Characterization of binding of *Candida albicans* to small intestinal mucin and its role in adherence to mucosal epithelial cells, Infect. Immun. 68 (6) (2000) 3172–3179.

[62] H.P. Felgueiras, N.S. Murthy, S.D. Sommerfeld, M.M. Brás, V. Migonney, J. Kohn, Competitive adsorption of plasma proteins using a quartz crystal microbalance, ACS Appl. Mater. Interfaces 8 (21) (2016) 13207–13217.

[63] T. Kamaya, Lytic action of lysozyme on *Candida albicans*, Mycopathol. Mycol. Appl. 42 (3) (1970) 197–207.

[64] K. Rezwan, L.P. Meier, L.J. Gauckler, Lysozyme and bovine serum albumin adsorption on uncoated silica and AlOOH-coated silica particles: the influence of positively and negatively charged oxide surface coatings, Biomaterials 26 (21) (2005) 4351–4357.
[65] J. Vörös, The density and refractive index of adsorbing protein layers, Biophys. J. 87 (1) (2004) 553–561.
[66] I. Van De Keere, S. Svedhem, H. Högberg, J. Vereecken, B. Kasemo, A. Hubin, In situ control of the oxide layer on thermally evaporated titanium and lysozyme adsorption by means of electrochemical quartz crystal microbalance with dissipation, ACS Appl. Mater. Interfaces 1 (2) (2009) 301–310.
[67] J. Su, Y. Sun, Z. Li, Y. Chen, B. Ding, W. Sun, Effect of tannic acid on lysozyme activity through intermolecular noncovalent binding, J. Agric. Food Res. 1 (2019), 100004.
[68] J.R. Lu, T.J. Su, P.N. Thirtle, R.K. Thomas, A.R. Rennie, R. Cubitt, The denaturation of lysozyme layers adsorbed at the hydrophobic solid/liquid surface studied by neutron reflection, J. Colloid Interface Sci. 206 (1) (1998) 212–223.
[69] D.M. Eby, H.R. Luckarift, G.R. Johnson, Hybrid antimicrobial enzyme and silver nanoparticle coatings for medical instruments, ACS Appl. Mater. Interfaces 1 (7) (2009) 1553–1560.
[70] S. Yang, Y. Wang, X. Wu, S. Sheng, T. Wang, X. Zan, Multifunctional tannic acid (TA) and lysozyme (Lys) films built layer by layer for potential application on implant coating, ACS Biomater. Sci. Eng. 5 (7) (2019) 3582–3594.
[71] F. Weber, H.Q. Quach, M. Reiersen, S.Y. Sarraj, D.N. Bakir, V.A. Jankowski, P. H. Nilsson, H. Tiainen, Characterization of the foreign body response of titanium implants modified with polyphenolic coatings, J. Biomed. Mater. Res. Part A 110 (7) (2022) 1341–1355.